Cite this: *INEOS OPEN*, **2023**, *6 (5)*, 144–149
DOI: 10.32931/io2324a

Received 26 January 2024,
Accepted 14 February 2024

http://ineosopen.org

POROUS ORGANIC POLYMERS BASED ON A POLYMER OF INTRINSIC MICROPOROSITY

I. I. Ponomarev, Yu. A. Volkova, E. S. Vtyurina, and K. M. Skupov*

Nesmeyanov Institute of Organoelement Compounds, Russian Academy of Sciences, ul. Vavilova 28, str. 1, Moscow, 119334 Russia

Abstract

The synthesis of porous organic polymers (POPs) based on a polymer of intrinsic microporosity (PIM), which represent a new class of promising materials, has been studied in detail. These porous systems are formed by precise joining of organic building blocks through covalent bonds in order to create predefined assemblies and can possess a three-dimensional (3D) or 2D-layered structure. The model reactions are considered and porosimetry studies are performed for the resulting POPs.

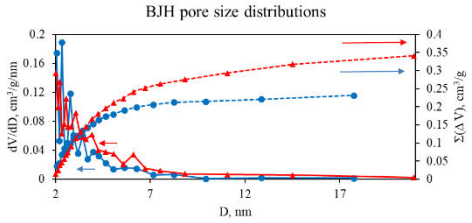

Key words: polyheteroarylene, PIM-1, gas separation membrane, porous organic polymer, microporosity.

Introduction

The development of modern fundamental science, in particular, polymer chemistry creates the basis and provides the latest breakthrough technologies for previously unknown substances and materials based on them. Without these technologies and materials, it is impossible to create fundamentally new miniature energy-saving and efficient devices operating at molecular level increasingly fast. Chemical design of new polymer heterocyclic molecules allows targeted modification and optimization of the physicochemical and functional properties of products such as coatings, films and fibers at the nanoscale. Nanostructured materials based on aromatic heterocyclic polymers are already widely represented in photovoltaics, membrane technologies, sensor devices, *etc*. The development of new recyclable molecules of heterocyclic polymers with a wide range of optical, thermal, gas separation, and other physical and chemical properties seems relevant at the current level of development of nanotechnology [1–8]. The polymer of intrinsic microporosity (PIM-1) was well studied in the last decade [1–3, 9–18]. It possesses unique gas separation properties and high specific surface area (up to 800 m^2/g). However, it is prone to aging and shows unstable gas separation properties, which could be eliminated by its chemical structuring with the obtainment of a covalent framework. It seems promising to synthesize and study a covalent organic framework [4–8] (COF)-like cross-linked porous polymer based on the typical monomer for PIM-1 synthesis (5,5',6,6'-tetrahydroxy-3,3,3',3'-tetramethylspiro-1,1'-bisindane, TTSBI), the product of its interaction with octafluorotoluene (28F-TTSBI) and 9,10-bis(4-fluorophenyl)-2,3,6,7-tetrakis[2,3,5,6-tetrafluoro-4-(trifluoromethyl)phenoxy]anthracene (30F-PA).

Earlier, we have shown for the first time that 30F-PA is formed under conditions of the PIM-1 synthesis from 2,3,6,7-tetrahydroxy-9,10-(*p*-fluorophenyl)anthracene in excess of octafluorotoluene (Scheme 1) [9].

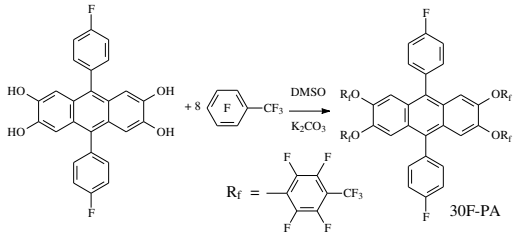

Scheme 1. Synthesis of 30F-PA.

Moreover, the full X-ray study of 30F-PA have been performed [9]. Then it was assumed that in 2,3,5,6-tetrafluoro-4-(trifluoromethyl)phenoxy-substituents at least two *ortho*-substituted fluorine atoms, activated by an acceptor trifluoromethyl group, would be able to react with catechols, producing dibenzodioxane rings. Similar reactions were observed earlier when pentafluorophenyl-substituted quinazolines reacted with catechol with quantitative yields (Scheme 2).

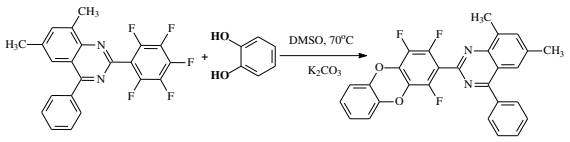

Scheme 2. Reaction of pentafluorophenyl-substituted quinazolines with catechol.

PIM-1 is a well-known polymer [10–18]. Our experience related to PIM-1 [19–26] suggests that the synthesis of PIM-1 is based on a very complex heterogeneous process of multistage polycyclocondensation of tetrafunctional monomers, which react according to the mechanism of nucleophilic aromatic substitution in an aprotic dipolar solvent medium. The known methods for producing PIM polymers need to be improved and

studied in-depth in terms of their optimization and various synthetic directions.

In the current study, the polycondensation activation processes are studied in detail for bis-catechols and polyfluoroaromatic activated monomers in the presence of K_2CO_3 in aprotic dipolar solvent media (such as DMSO) using ultrasound. The resulting COF-like porous organic polymers (POPs) are studied in detail by N_2 low-temperature (77 K) adsorption to obtain their specific volume (SV) and specific surface area (SSA) values and assess their microporosity by the t-method. Up to our knowledge, such studies have been never performed before for the polyheterocyclization reactions under nucleophilic aromatic substitution reaction conditions.

Results and discussion

Syntheses

The main difference between the current study and most other works devoted to the PIM synthesis is that the process of multistage PIM-1 polycyclocondensation of tetrafunctional monomers, which is accomplished according to the mechanism of nucleophilic aromatic substitution and proceeds as a precipitation reaction in DMSO [19, 20] (an aprotic dipolar solvent classified as a green solvent), is used to obtain insoluble assumably cross-linked POPs.

The precipitation polyheterocyclization does not always lead to high-molecular polymers of a linear structure. Therefore, the optimization of such a process requires precise adjustment of all parameters which include: the reaction temperature, the concentration of monomers, the concentration of acceptor catalyst, the amount of releasing low-molecular weight product (in our case, HF which binds with K_2CO_3 to form KF), the order of reagent addition, and some other parameters.

To prove the feasibility of this type of reactions, the first model compound, 1-(3-chlorophenoxy)-2,3,5,6-tetrafluoro-4-(trifluoromethyl)benzene, was synthesized. Then it was introduced into reaction with catechol to obtain the second model compound—1-(3-chlorophenoxy)-2,3-difluoro-4-(trifluoromethyl)dibenzo[b,e][1,4]dioxin (Scheme 3).

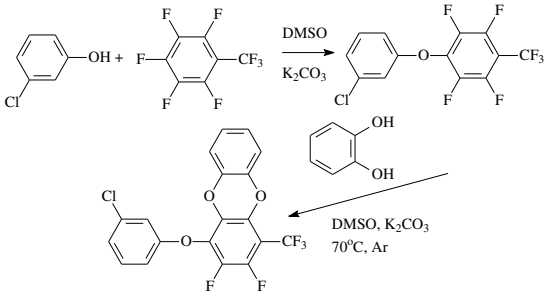

Scheme 3. Synthesis of the model compounds.

The model compounds were obtained in high yields (>95%) and were characterized by the ^{1}H NMR spectroscopic data and elemental analyses. The results obtained strongly confirmed the possibility of producing POPs based on polyfluoroaromatic compounds.

Two POPs were synthesized. Sample **1** was synthesized from TTSBI and 30F-PA (Scheme 4), while sample **2** was synthesized from TTSBI and 28F-TTSBI (Scheme 5).

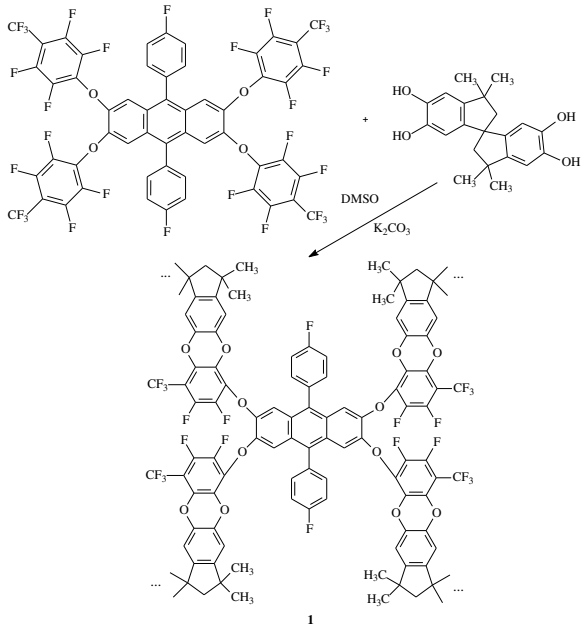

Scheme 4. Synthesis of **1**.

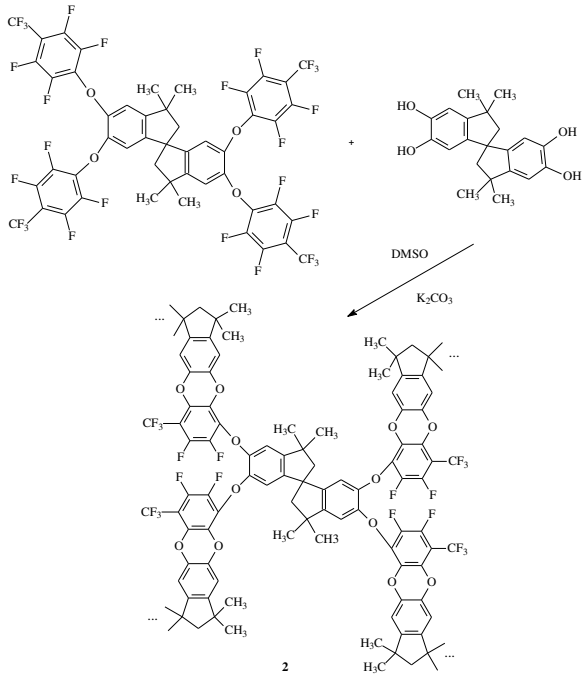

Scheme 5. Synthesis of **2**.

Two fluorinated monomers can react with TTSBI in 1:2 molar ratio with the formation of insoluble porous organic polymers **1** and **2**, cross-linked in four directions, in 94% and 95% yields, respectively. The corresponding fluorine content was observed according to the elemental analysis. If the reaction was not complete, evidently, the insoluble fraction would be sufficiently lower and the higher fluorine content would be observed.

Nitrogen adsorption studies

The resulting POPs are stable ordered substances, obtained by the reaction of the organic precursors with the formation of new covalent bonds. In addition, they possess a porous structure which consists of micropores (<2 nm), mesopores (2–50 nm),

and macropores (>50 nm). Some of the most important characteristics of POPs are their porosimetry properties, which make possible to determine the SV and SSA values of a porous system, as well as to obtain pore size distribution and to take into account the contribution of micropores.

In the current study, the investigations of the resulting POPs (**1** and **2**) were carried out by low-temperature (77 K) nitrogen adsorption at 0–0.1 MPa. The adsorption isotherms were obtained as the dependences of the adsorbed nitrogen specific volume, V (in cm^3 per 1 g of the sample at a standard temperature and pressure (IUPAC STP [27]): 273 K, 100 kPa)) *vs.* relative pressure, p/p_0, where p is an equilibrium pressure and p_0 is the nitrogen saturated vapor pressure (1 atm in our case). To obtain the SV and SSA values, the Brunauer–Emmett–Teller (BET) theory in combination with the t-method were applied to the low-temperature adsorption isotherms. By this way, the SSA (S_{BET}), micropore SV (V_μ), micropore SSA (S_μ), as well as macro- and mesopore SSA (S_{mm}) were calculated. The total specific pore volume (V_t) was determined at p/p_0 = 0.99 (for pore sizes < ~200 nm). The resulting adsorption isotherms for **1** and **2** are depicted in Fig. 1.

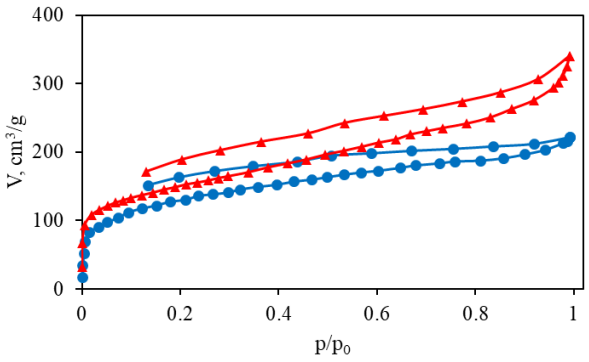

Figure 1. Nitrogen low-temperature (77 K) adsorption–desorption isotherms for **1** (circles, blue) and **2** (triangles, red).

The shape of the isotherms is close to type II. The desorption branches suggest the presence of microporosity. To find the values of S_{BET}, the BET plots, limited by p/p_0 = 0.18 according to the Rouquerol criteria [28], were plotted (Fig. 2).

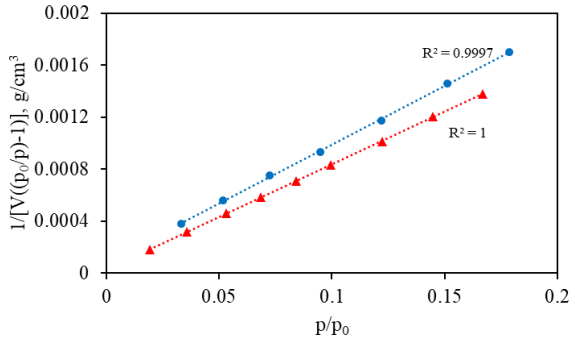

Figure 2. BET plots for **1** (circles, blue) and **2** (triangles, red).

To obtain the values of V_μ, S_μ, and S_{mm}, the t-method was applied using the Harkins–Jura equation [29, 30] for the adsorption layer thickness (t) in the range of 0.45–0.65 nm: t(nm) = $[13.99/(0.034–\log(p/p_0))]^{0.5}$. The corresponding t-plots for V_μ, S_μ, and S_{mm} determination are provided in Fig. 3 (for the full-range t-plots, see the Electronic supplementary information (ESI)).

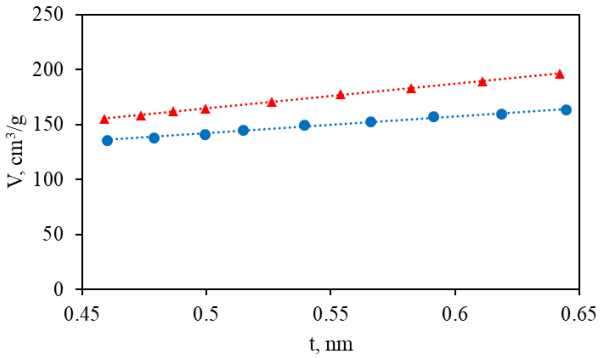

Figure 3. t-Plots for **1** (circles, blue) and **2** (triangles, red).

The SSA and SV values as well as the pore size values for **1** and **2** are listed in Table 1.

Table 1. Specific surface area, volume values, and pore sizes for **1** and **2**

POP	S_{BET}, m^2/g	S_μ, m^2/g	S_{mm}, m^2/g	V_μ, cm^3/g	V_t, cm^3/g	d, nm[a]
1	476	241	235	0.103	0.341	2.9
2	536	191	345	0.082	0.519	3.9

[a]the average pore diameter was calculated as $d = 4V_t/S_{BET}$.

As can be seen from Table 1, total SSA (S_{BET}) for **2** is higher than that for **1** (536 *vs.* 476 m^2/g). Similarly, a higher value of total SV (V_t) is observed (0.519 *vs.* 0.341 cm^3/g for the pore sizes < ~200 nm). At the same time, SSA of micropores (S_μ) and SV of micropores (V_μ) for **2**, on the contrary, are lower compared to those for **1** (191 and 241 m^2/g, 0.082 and 0.103 cm^3/g, respectively), whereas for macro- and mesopores, the SSA value (S_{mm}) for **2** is higher than that for **1** (345 and 235 m^2/g, respectively). The data obtained indicate that higher total values of SSA and SV for **2** compared with those for **1** are achieved due to a higher fraction of macro- and mesopores and a decrease in the SSA and SV of micropores. It is also confirmed by the higher value of the average pore diameter (d) for **2** compared with that for **1** (3.9 and 2.9 nm, respectively). The integral and differential pore size distributions for mesopores obtained by the Barrett–Joyner–Halenda (BJH) method in the range of 2–20 nm also confirm this conclusion (Fig. 4).

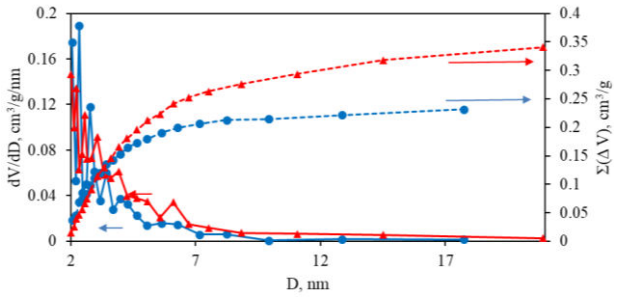

Figure 4. Integral (dotted lines) and differential (solid lines) mesopore size distribution curves according to the BJH method for **1** (circles, blue) and **2** (triangles, red).

As can be seen from Fig. 4, the SV value of mesopores is higher for **2** than for its counterpart **1**. It is also obvious from the

pore size distribution curves that the mesopore SV value for **2** becomes higher for mesopores with D > 3 nm, while the mesopore SV for mesopores with D < 3 nm is slightly higher for **1**. Thus, combining the BJH results with the results of the t-method and BET analysis, it can be concluded that the higher discussed values for **2** compared with those for **1** are achieved due to a larger proportion of macro- and mesopores with a size of D > 3 nm in **2**.

Experimental section

General remarks

5,5',6,6'-Tetrahydroxy-3,3,3',3'-tetramethyl-1,1'-spirobisindane (TTSBI, 97%) was obtained from TCI Europe (Zwijndrecht, Belgium). 3-Chlorophenol (>98%), catechol (>98%), and dimethyl sulfoxide (≥99%) were obtained from Acrus (Moscow, Russia). Octafluorotoluene (99%) was obtained from P&M (Moscow, Russia). K_2CO_3 (>99.5%) from Acrus (Moscow, Russia) was dried overnight at 160 °C.

Syntheses

Synthesis of 9,10-bis(4-fluorophenyl)-2,3,6,7-tetrakis[2,3,5,6-tetrafluoro-4-(trifluoromethyl)phenoxy]-anthracene (30F-PA). The detailed synthetic procedure for 30F-PA is provided in Ref. [9]. Briefly, 1.900 g (8 mmol) of octafluorotoluene, 0.861 g (2 mmol) of 2,3,6,7-tetrahydroxy-9,10-di(p-fluorophenyl)anthracene, 1.100 g (8 mmol) of K_2CO_3, 8 mL of DMSO, and 2 mL of toluene were stirred under an argon atmosphere starting at room temperature with sonification and then at 80 °C for 5 h. Yield: 77%. Anal. Calcd for $C_{54}H_{12}F_{30}O_4$: C, 50.10; H, 0.93; F, 44.02. Found: C, 50.5; H, 0.83; F, 43.93%. T_m = 256 – 259 °C. MW = 1294.6 g/mol.

5,5',6,6'-Tetrakis[2,3,5,6-tetrafluoro-4-(trifluoromethyl)-phenoxy]-3,3,3',3'-tetramethyl-1,1' spirobisindane (28F-TTSBI). 0.681 g (2 mmol) of 5,5',6,6'-tetrahydroxy-3,3,3',3'-tetramethyl-1,1'-spirobisindane, 1.900 g (8 mmol) of octafluorotoluene, 1.100 g (8 mmol) of K_2CO_3, 8 mL of DMSO, and 2 mL of toluene were charged into a flask under an argon flow at room temperature. The stirred reaction mixture was placed into an Elmasonic S 10 (H) ultrasonic bath (Elma Schmidbauer, Singen, Germany) pre-heated to 80 °C with non-stop sonification at 37 kHz for 5 h. Then, DI water (30 mL) was added to the reaction mixture and heating was continued under sonification for 30 min to remove all inorganic substances. The filtration followed by drying afforded 2.0 g of the target product as white crystals. Yield: 83%. Anal. Calcd for $C_{49}H_{20}F_{28}O_4$: C, 48.86; H, 1.67; F, 44.16. Found: C, 49.15; H, 1.78; F, 44.66%. MW = 1204.65 g/mol.

Synthesis of 1-(3-chlorophenoxy)-2,3,5,6-tetrafluoro-4-(trifluoromethyl)benzene.

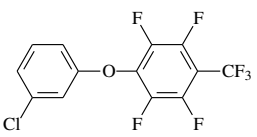

1.29 g (10 mmol) of 3-chlorophenol, 3 mL (> 20 mmol) of octafluorotoluene, 1.38 g of K_2CO_3, 5 mL of DMSO, and 1 mL of toluene were charged into a flask under an argon flow at room temperature. The stirred reaction mixture was placed into an Elmasonic S 10 (H) ultrasonic bath (Elma Schmidbauer, Singen, Germany) pre-heated to 80 °C with non-stop sonification at 37 kHz for 4 h. Then, DI water (30 mL) was added to the reaction mixture and it was heated under sonification at 80 °C for 30 min to remove all inorganic substances. The liquid product was separated from the aqueous phase. Yield: 3.00 g (87%). Anal. Calcd for $C_{13}H_4ClF_7O$: C, 45.31; H, 1.17; F, 38.59. Found: C, 45.35; H, 1.48; F, 38.56%. MW = 344.62 g/mol.

Synthesis of 1-(3-chlorophenoxy)-2,3-difluoro-4-(trifluoromethyl)dibenzo[b,e][1,4]dioxin.

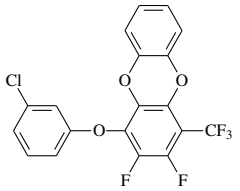

2.353 g (6.83 mmol) of 1-(3-chlorophenoxy)-2,3,5,6-tetrafluoro-4-(trifluoromethyl)benzene, 0.800 g (7.30 mmol) of catechol, 1.900 g (14.00 mmol) of K_2CO_3, 5 mL of DMSO, and 1 mL of toluene were charged into a flask under an argon flow at room temperature. The stirred reaction mixture was placed into an Elmasonic S 10 (H) ultrasonic bath (Elma Schmidbauer, Singen, Germany) pre-heated to 80 °C with non-stop sonification at 37 kHz for 6 h. Then, DI water (50 mL) was added to the reaction mixture and heated under sonification at 80 °C for 30 min to remove all inorganic substances. The filtration followed by drying afforded the target product as white crystals. T_m = 85–86 °C. Yield: 2.820 g (98%). Anal. Calcd for $C_{19}H_8ClF_5O_3$: C, 55.03; H, 1.94; F, 22.91. Found: C, 55.31; H, 1.98; F, 22.59%. MW = 414.72 g/mol.

Preparation of sample 1. 0.2589 g (0.2 mmol) of 9,10-bis(4-fluorophenyl)-2,3,6,7-tetrakis[2,3,5,6-tetrafluoro-4-(trifluoromethyl)phenoxy]anthracene, 0.1362 g (0.4 mmol) of 5,5',6,6'-tetrahydroxy-3,3,3',3'-tetramethyl-1,1'-spirobisindane, 0.2500 g (1.8 mmol) of K_2CO_3, 4 mL of DMSO, and 0.5 mL of toluene were charged into a flask under an argon flow at room temperature. The stirred reaction mixture was placed into an Elmasonic S 10 (H) ultrasonic bath (Elma Schmidbauer, Singen, Germany) pre-heated to 80 °C with non-stop sonification at 37 kHz for 4 h and without sonification at 150 °C for 4 h. Then, DI water (30 mL) was added to the reaction mixture and heated under sonification at 80 °C for 30 min to remove all inorganic substances. The filtration followed by drying afforded 0.3300 g of the target product as a white powder. Yield: 94%. Anal. Calcd for $C_{106}H_{68}F_{22}O_{12}$: C, 65.23; H, 3.51; F, 21.42. Found: C, 65.85; H, 3.83; F, 22.93%. M(unit) = 1951.7 g/mol.

Preparation of sample 2. 0.1205 g (0.1 mmol) of 5,5',6,6'-tetrakis[2,3,5,6-tetrafluoro-4-(trifluoromethyl)phenoxy]-3,3,3',3'-tetramethyl-1,1'-spirobisindane (28F-TTSBI), 0.0681 g (0.2 mmol) of 5,5',6,6'-tetrahydroxy-3,3,3',3'-tetramethyl-1,1'-spirobisindane, 0.1200 g (0.9 mmol) of K_2CO_3, 1.5 mL of DMSO, and 0.2 mL of toluene were charged into a flask under an argon flow at room temperature. The stirred reaction mixture was placed into an Elmasonic S 10 (H) ultrasonic bath (Elma Schmidbauer, Singen, Germany) pre-heated to 80 °C with non-stop sonification at 37 kHz for 4 h and without sonification at 150 °C for 4 h. Then, DI water (30 mL) was added to the

reaction mixture and heated under sonification at 80 °C for 30 min to remove all inorganic substances. The filtration followed by drying afforded 0.1500 g of the target product as a white powder. Yield: 95%. Anal. Calcd for $C_{101}H_{76}F_{20}O_{12}$: C, 65.16; H, 4.11; F, 20.41. Found: C, 65.85; H, 3.83; F, 19.93%. M(unit) = 1861.7 g/mol.

Nitrogen adsorption studies

The low-temperature nitrogen adsorption isotherms (77 K) were obtained on a 3P Micro 200 Surface Area and Pore Size Analyzer (3P Instruments, Odelzhausen, Germany) in the range of 0.001–1 bar. To determine SSA (S_{BET}), the BET equation was applied to the nitrogen adsorption isotherm data in the range of relative pressure values limited by the Rouquerol criteria [28]. For calculations, adsorbed N_2 density was taken as 0.808 g·mL^{-1} and N_2 cross-sectional area was taken as 0.162 nm^2. The SSA and SV of micropores (S_μ and V_μ) and the SSA of meso- and macropores (S_{mm}) were found by applying the t-method with the Harkins–Jura equation [29, 30] for the thickness layer in the range of adsorption thickness (t) of 0.45–0.65 nm. The total pore volume (V_{tot}) was determined from the adsorbed nitrogen amount at a relative pressure (p/p_0) of 0.990. The average pore diameter (d) was calculated as $4V_{tot}/S_{BET}$. The pore size distributions of mesopores were obtained from the isotherm adsorption branches by the BJH method.

Conclusions

The process of the new POP synthesis based on 9,10-bis(4-fluorophenyl)-2,3,6,7-tetrakis[2,3,5,6-tetrafluoro-4-(trifluoromethyl)phenoxy]anthracene, 5,5',6,6'-tetrahydroxy-3,3,3',3'-tetramethylspiro-1,1'-bisindane and the product of its interaction with octafluorotoluene (28F-TTSBI) was studied for the first time. Furthermore, the POP with a PIM-like linker was obtained. The model reactions and the porosimetry studies were performed for resulting samples **1** and **2**. Based on the results of the low-temperature nitrogen adsorption (77 K) using the BET, BJH, and t-methods for the isotherm analysis, it was shown that the samples possess micro- and mesoporosity. It was found that **2** possesses higher total specific surface area and specific volume values. However, the micropore specific surface area and micropore specific volume for **2** are lower than those for **1**. The data obtained indicate a higher contribution of the pores with D > 3 nm in the total porosity of **2**.

Acknowledgements

This work was performed with financial support from the Ministry of Science and Higher Education of the Russian Federation (agreement no. 075-00277-24-00) using the equipment of the Center for Molecular Composition Studies of INEOS RAS.

Corresponding author

* E-mail: kskupov@ineos.ac.ru. Tel. +7 (499)135-9276, ext. 1137 (K. M. Skupov)

Electronic supplementary information

Electronic supplementary information (ESI) available online: the NMR spectra and full range t-plots. For ESI, see DOI: 10.32931/io2324a.

References

1. N. B. McKeown, *Sci. China: Chem.*, **2017**, *60*, 1023–1032. DOI: 10.1007/s11426-017-9058-x
2. P. M. Budd, B. S. Ghanem, S. Makhseed, N. B. McKeown, K. J. Msayib, C. E. Tattershall, *Chem. Commun.*, **2004**, 230–231. DOI: 10.1039/b311764b
3. C. G. Bezzu, M. Carta, M.-C. Ferrari, J. C. Jansen, M. Monteleone, E. Esposito, A. Fuoco, K. Hart, T. P. Liyana-Arachchi, C. M. Colina, N. B. McKeown, *J. Mater. Chem. A*, **2018**, *6*, 10507–10514. DOI: 10.1039/C8TA02601G
4. Y. Zeng, R. Zou, Y. Zhao, *Adv. Mater.*, **2016**, *28*, 2855–2873. DOI: 10.1002/adma.201505004
5. S. Kandambeth, B. P. Biswal, H. D. Chaudhari, K. C. Rout, S. Kunjattu H., S. Mitra, S. Karak, A. Das, R. Mukherjee, U. K. Kharul, R. Banerjee, *Adv. Mater.*, **2017**, *29*, 1603945. DOI: 10.1002/adma.201603945
6. Y. Du, H. Yang, J. M. Whiteley, S. Wan, Y. Jin, S.-H. Lee, W. Zhang, *Angew. Chem., Int. Ed.*, **2016**, *55*, 1737–1741. DOI: 10.1002/anie.201509014
7. S.-Y. Ding, J. Gao, Q. Wang, Y. Zhang, W.-G. Song, C.-Y. Su, W. Wang, *J. Am. Chem. Soc.*, **2011**, *133*, 19816–19822. DOI: 10.1021/ja206846p
8. H. Li, Q. Pan, Y. Ma, X. Guan, M. Xue, Q. Fang, Y. Yan, V. Valtchev, S. Qiu, *J. Am. Chem. Soc.*, **2016**, *138*, 14783–14788. DOI: 10.1021/jacs.6b09563
9. I. I. Ponomarev, K. M. Skupov, K. A. Lyssenko, I. V. Blagodatskikh, A. V. Muranov, Yu. A. Volkova, D. Yu. Razorenov, Iv. I. Ponomarev, L. E. Starannikova, D. A. Bezgin, A. Yu. Alentiev, Yu. P. Yampolskii, *Mendeleev Commun.*, **2020**, *30*, 734–737. DOI: 10.1016/j.mencom.2020.11.015
10. Z.-X. Low, P. M. Budd, N. B. McKeown, D. A. Patterson, *Chem. Rev.*, **2018**, *118*, 5871–5911. DOI: 10.1021/acs.chemrev.7b00629
11. N. B. McKeown, *Polymer*, **2020**, *202*, 122736. DOI: 10.1016/j.polymer.2020.122736
12. Y. Liu, J. Zhang, X. Tan, *ACS Omega*, **2019**, *4*, 16572–16577. DOI: 10.1021/acsomega.9b02363
13. S. Thomas, I. Pinnau, N. Du, M. D. Guiver, *J. Membr. Sci.*, **2009**, *333*, 125–131. DOI: 10.1016/j.memsci.2009.02.003
14. A. B. Foster, J. L. Beal, M. Tamaddondar, J. M. Luque-Alled, B. Robertson, M. Mathias, P. Gorgojo, P. M. Budd, *J. Mater. Chem. A*, **2021**, *9*, 21807–21823. DOI: 10.1039/D1TA03712A
15. P. M. Budd, N. B. McKeown, B. S. Ghanem, K. J. Msayib, D. Fritsch, L. Starannikova, N. Belov, O. Sanfirova, Yu. Yampolskii, V. Shantarovich, *J. Membr. Sci.*, **2008**, *325*, 851–860. DOI: 10.1016/j.memsci.2008.09.010
16. P. M. Budd, K. J. Msayib, C. E. Tattershall, B. S. Ghanem, K. J. Reynolds, N. B. McKeown, D. Fritsch, *J. Membr. Sci.*, **2005**, *251*, 263–269. DOI: 10.1016/j.memsci.2005.01.009
17. C. L. Staiger, S. J. Pas, A. J. Hill, C. J. Cornelius, *Chem. Mater.*, **2008**, *20*, 2606–2608. DOI: 10.1021/cm071722t
18. L. Wang, Y. Zhao, B. Fan, M. Carta, R. Malpass-Evans, N. B. McKeown, F. Marken, *Electrochem. Commun.*, **2020**, *118*, 106798. DOI: 10.1016/j.elecom.2020.106798
19. I. I. Ponomarev, I. V. Blagodatskikh, A. V. Muranov, Yu. A. Volkova, D. Yu. Razorenov, Iv. I. Ponomarev, K. M. Skupov, *Mendeleev Commun.*, **2016**, *26*, 362–364. DOI: 10.1016/j.mencom.2016.07.033
20. I. I. Ponomarev, I. V. Blagodatskikh, A. V. Muranov, Yu. A. Volkova, D. Yu. Razorenov, Iv. I. Ponomarev, K. M. Skupov, *Polym. Sci., Ser. C*, **2020**, *62*, 259–265. DOI: 10.1134/S1811238220020113

21. K. M. Skupov, I. I. Ponomarev, D. Y. Razorenov, V. G. Zhigalina, O. M. Zhigalina, Iv. I. Ponomarev, Yu. A Volkova, Yu. M. Volfkovich, V. E. Sosenkin, *Macromol. Symp.*, **2017**, *375*, 1600188. DOI: 10.1002/masy.201600188
22. I. I. Ponomarev, K. M. Skupov, Iv. I. Ponomarev, D. Yu. Razorenov, Yu. A. Volkova, V. G. Basu, O. M. Zhigalina, S. S. Bukalov, Yu. M. Volfkovich, V. E. Sosenkin, *Russ. J. Electrochem.*, **2019**, *55*, 552–557. DOI: 10.1134/S1023193519060156
23. I. I. Ponomarev, K. A. Lyssenko, D. Yu. Razorenov, Yu. A. Volkova, Iv. I. Ponomarev, K. M. Skupov, Z. S. Klemenkova, L. E. Starannikova, A. Yu. Alentiev, Yu. P. Yampolskii, *Mendeleev Commun.*, **2019**, *29*, 663–665. DOI: 10.1016/j.mencom.2019.11.020
24. A. Yu. Alentiev, D. A. Bezgin, L. E. Starannikova, R. Yu. Nikiforov, I. I. Ponomarev, Yu. A. Volkova, K. M. Skupov, I. A. Ronova, Yu. P. Yampolskii, *Membr. Membr. Technol.*, **2021**, *3*, 199–205. DOI: 10.1134/S2517751621040028
25. I. I Ponomarev, Yu. A. Volkova, Iv. I. Ponomarev, D. Y. Razorenov, K. M. Skupov, R. Y. Nikiforov, S. V. Chirkov, V. E. Ryzhikh, N. A. Belov, A. Y. Alentiev, *Polymer*, **2022**, *238*, 124396. DOI: 10.1016/j.polymer.2021.124396
26. K. M. Skupov, E. S. Vtyurina, I. I. Ponomarev, Iv. I. Ponomarev, R. R. Aysin, *Polymer*, **2023**, *264*, 125546. DOI: 10.1016/j.polymer.2022.125546
27. M. B. Ewing, T. H. Lilley, G. M. Olofsson, M. T. Ratzsch, G. Somsen, *Pure Appl. Chem.*, **1994**, *66*, 533–552. DOI: 10.1351/pac199466030533
28. F. Rouquerol, J. Rouquerol, K. S. W. Sing, P. Llewellyn, G. Maurin, *Adsorption by Powders and Porous Solids: Principles, Methodology and Applications*, *2nd ed*., Acad. Press, Oxford, **2012**. DOI: 10.1016/C2010-0-66232-8
29. W. D. Harkins, G. Jura, *J. Am. Chem. Soc.*, **1944**, *66*, 1362–1366. DOI: 10.1021/ja01236a047
30. J. Choma, M. Jaroniec, M. Kloske, *Adsorpt. Sci. Technol.*, **2002**, *20*, 307–315. DOI: 10.1260/026361702760254487